Blood First Edition Paper, prepublished online June 20, 2017; DOI 10.1182/blood-2017-03-776070

SF3B1-Initiating Mutations in MDS with Ring Sideroblasts Target Lymphomyeloid Hematopoietic Stem Cells

Teresa Mortera-Blanco,[1] Marios Dimitriou,[1] Petter S Woll,[1,2] Mohsen Karimi,[1] Edda Elvarsdottir,[1] Simona Conte,[1] Magnus Tobiasson,[1] Monika Jansson,[1] Iyadh Douagi,[1] Matahi Moarii,[3] Leonie Saft,[4] Elli Papaemmanuil,[3] Sten Eirik W Jacobsen,[1,2*] Eva Hellström-Lindberg[1*]

[1]Center for Hematology and Regenerative Medicine, Karolinska Institutet, Department of Medicine, Karolinska University Hospital Huddinge, Stockholm, Sweden. [2]Haematopoietic Stem Cell Biology Laboratory, MRC Molecular Haematology Unit, Weatherall Institute of Molecular Medicine, University of Oxford, Oxford, UK. [3]Memorial Sloan Kettering Cancer Center, New York, NY, USA. [4]Department of Pathology, Division of Hematopathology, Karolinska University Hospital, Solna, Sweden

* S.E.W.J and E.H.L contributed equally to this study

Correspondence: Eva Hellström-Lindberg, Karolinska Institute, Department of Medicine, Center for Hematology and Regenerative Medicine, Karolinska University Hospital Huddinge, 141 86 Stockholm, Sweden; email: eva.hellstrom-lindberg@ki.se.
Sten Eirik W. Jacobsen, Karolinska Institute, Department of Medicine, Center for Hematology and Regenerative Medicine, Karolinska University Hospital Huddinge, 141 86 Stockholm, Sweden; email: sten.eirik.jacobsen@ki.se.

Running title: *SF3B1* mutation arises at the multipotent HSC level.

Word count Text: 3464 words; Abstract: 237 words

Number of figures: 4; Tables: 1

References: 43

Scientific category: Hematopoiesis and Stem Cells

Key Points:

- *SF3B1* mutations in MDS-RS have a multipotent lymphomyeloid origin.
- Transplantation of *SF3B1* mutated MDS-RS HSCs into immune-deficient mice results in generation of characteristic ring sideroblasts.

Abstract

Mutations in the RNA splicing gene *SF3B1* are found in more than 80% of patients with myelodysplastic syndrome with ring sideroblasts (MDS-RS). We investigated the origin of *SF3B1* mutations within the bone marrow hematopoietic stem and progenitor cell compartments in patients with MDS-RS. Screening for recurrently mutated genes in the mononuclear cell fraction revealed mutations in *SF3B1* in 39 of 40 cases (97.5%), combined with *TET2* and *DNMT3A* in 11 (28%) and 6 (15%) patients, respectively. All recurrent mutations identified in mononuclear cells could be tracked back to the phenotypically defined hematopoietic stem cell (HSC) compartment in all investigated patients, and were also present in downstream myeloid and erythroid progenitor cells. While in agreement with previous studies little or no evidence for clonal (*SF3B1* mutation) involvement could be found in mature B cells, consistent involvement at the pro-B cell progenitor stage was established, providing definitive evidence for *SF3B1* mutations targeting lymphomyeloid HSCs, and compatible with mutated *SF3B1* negatively affecting lymphoid development. Assessment of stem cell function *in vitro* as well as *in vivo* established that only HSCs and not investigated progenitor populations could propagate the *SF3B1* mutated clone. Upon transplantation into immune-deficient mice, *SF3B1* mutated MDS-RS HSCs differentiated into characteristic ring sideroblasts, the hallmark of MDS-RS. Our findings provide evidence of a multipotent lymphomyeloid HSC origin of *SF3B1* mutations in MDS-RS patients, and provide a novel *in vivo* platform for mechanistically and therapeutically exploring *SF3B1* mutated MDS-RS.

Introduction

The pathogenesis of myelodysplastic syndromes (MDS) involves a spectrum of genetic alterations and varies considerably between disease subgroups.[1] Recurrent mutations in lower-risk MDS are largely confined to core components of the spliceosome (*SF3B1, SRSF2, U2AF35* and *ZRSR2*), epigenetic modifiers (*TET2, DNMT3A*, *IDH1/2*, *ASXL1*), and genes involved in pathways such as signal transduction and transcriptional regulation.[2-4] While many mutations co-exist with each other and may be found in various myeloid malignancies, splice factor mutations occur in a mutually exclusive manner and are much more frequent than in other hematological tumors.[5,6] Remarkably, highly recurrent heterozygous mutations in the RNA splicing gene *SF3B1* are found in as many as 70-85% of patients with lower-risk MDS and ring sideroblasts (MDS-RS),[2,3,7] but are relatively rare in other MDS subtypes. Recurrent *SF3B1* mutations are therefore likely to play a distinct biological role in MDS-RS pathogenesis.[8] Other studies have identified recurrent *SF3B1* mutations in otherwise healthy elderly individuals, as evidence for *SF3B1* mutations also being involved in pre-malignant clonal hematopoiesis.[9]

In MDS-RS mitochondrial ferritin accumulates in the mitochondria of the erythroblasts resulting in accumulation of characteristic ring sideroblasts (RS), ineffective erythropoiesis, and anemia. We previously reported that MDS-RS erythroblasts display reduced expression of *ABCB7*, a gene involved in the regulation of mitochondrial iron homeostasis, and that the expression level of *ABCB7* is inversely associated with the percentage of marrow RS. We also demostrated that *SF3B1* mutated MDS-RS progenitors display impaired splicing with potential downstream consequences for genes of key importance for hemoglobin synthesis and terminal erythroid differentiation.[10] Although these and other findings implicate an impact of recurrent *SF3B1* mutations primarily in the erythroid lineage, the primary cellular target(s) of these recurrent *SF3B1* mutations remain to be elucidated. While having a low propensity for leukemic transformation, these patients typically suffer from severe anemia requiring regular transfusion

therapy, and there is currently no curative treatment available for them.[11] Importantly, in addition to negatively affecting erythroid lineage development, recurrent *SF3B1* mutations provide a competitive clonal advantage in MDS-RS, but it remains unclear at which level in the hematopoietic hierarchy this advantage is achieved. Establishing this, as well as the identity of the hematopoietic cells capable of propagating and sustaining the *SF3B1*-mutated clone, will be key towards developing more targeted and potentially curative therapeutic strategies for *SF3B1*-mutated MDS-RS. Recent studies have suggested that *SF3B1* mutations might primarily target the phenotypic hematopoietic stem cell (HSC) compartment.[12] However, it is widely recognized that any phenotypically defined HSC population also contains a substantial fraction of non-HSCs, and since the lymphoid lineages were not found to be involved in the *SF3B1*-mutated clones,[3,12,13] definitive evidence for recurrent *SF3B1* mutations targeting true lymphomyeloid HSCs in MDS-RS are lacking.

Here, we provide evidence that recurrent *SF3B1* mutations target the multipotent lymphomyeloid HSC compartment and that only these targeted HSCs are able to long-term propagate the *SF3B1*-mutated clone *in vitro* and *in vivo.* Importantly, we also demonstrate in immune-deficient mice the *in vivo* differentiation of purified HSCs from *SF3B1*-mutated MDS-RS patients to characteristic RS, providing a valuable *in vivo* platform for unraveling and targeting the dysregulated erythroid development in *SF3B1*-mutated MDS-RS.

Materials and Methods

Patient samples

Bone marrow (BM) and peripheral blood (PB) samples were obtained before treatment of MDS-RS patients, as defined in the WHO 2016 revision to the World Health Organization classification of myeloid neoplasms and acute leukemia, diagnosed using a multi-professional conference approach.[14] BM and PB were collected from 15 healthy subjects in the Hematology Department

at Karolinska University Hospital, Sweden. Informed consent was obtained from patients and healthy controls and the study was approved by the Ethics Research Committee at Karolinska Institutet (2010/427-31/1 and 2011/1257-31). BM mononuclear cells (MNC) were isolated by Lymphoprep (Fresenius, Oslo, Norway) gradient centrifugation.

Flow cytometry and fluorescent-activated cell sorting (FACS)

Stem and progenitor cells, mature lymphoid, myeloid and erythroid cells as well as NOD/LtSz-scid IL2Rγc$^{-/-}$ (NSG) human engraftment analysis and purification was performed as described in supplementary methods.

Functional stem and progenitor cell assays

Detailed methods for colony-forming cell (CFC) and long-term colony forming cell (LTC-CFC) assays are described in supplementary methods.

DNA mutational analysis

Targeted DNA sequencing of DNA isolated from the bulk BM from all 40 subjects was performed using Haloplex selector probes[15] and prepared according to manufacturer's instructions (Agilent, Santa Clara, CA, USA). The sequencing platform and mutational call analysis has been previously described,[15] and is also explained briefly in supplementary methods. For a number of patients, computational prediction analysis was performed as previously described for the targeted sequenced samples.[16] Briefly: After identifying and selecting the reliable driver mutations, we corrected the variant allele frequency (VAF) for gene mutations mapping on the X chromosome for the patients. We also assessed loss of heterozygosity (LoH) for genes such that the 95% confidence interval (CI) of the estimated VAF is higher than 65%. The distribution of the VAF is drawn from a beta-binomial distribution with the parameters number of mutated reads N_{mut} and the number of unmutated reads $N_{ref} = N_{tot} - N_{mut}$ and corrected the VAF

accordingly as previously described.[16] We then assessed precedence between gene mutations for each patient by comparing the 95% CI of VAF between genes.

To identify mutations in LTC-CFCs and CFCs colonies, genomic DNA from individual colonies was isolated using isopropanol/ethanol precipitation. Pyrosequencing was applied to detect the heterozygous *SF3B1* single nucleotide mutations previously found by targeted sequencing using Pyromark Q24 system (Qiagen, Hilden, Germany). DNA from healthy normal bone marrow (NBM) LTC-CFCs and CFCs was used as wild-type control. The colonies were only scored as positive or negative due to their assumed clonal origin. However, as there is a potential for contamination of cells from other colonies when picking colonies, we considered the colonies with a VAF above 25% as positive; those with a VAF below 5% as negative; and colonies with VAF between 6 to 24% as inconclusive. See supplementary methods for a more detailed description.

To quantify mutations in purified stem and progenitor cells we subjected isolated DNA to whole genome amplification using a Genomi-PHI V2 kit according to the manufacturer's instructions (GE Healthcare, Chicago, Illinois, USA). For pro-B cells we performed pyrosequencing to identify the mutations previously found by targeted sequencing, and to analyze the rest of the populations we used the Sequenom platform according to manufacturer's instructions at the mutational analysis facility (MAF) Karolinska Institute, Stockholm. Briefly, the assays were set up in multiplexed reactions with primer pairs designed to amplify the desired point mutations. The PCR reaction was then cleaned up by enzymatic reaction and extension primers were designed to anneal directly adjacent to the point mutation of interest. The extended primers were then subjected to MALDI-TOF (matrix-assisted laser desorption/ionization time of flight spectrometry) analysis on Sequenom MassARRAY® Analyzer (Agena Bioscience, San Diego, CA, USA). For the allelic discrimination and quantitative estimation of the mutated allelic frequency the SpectroTyper 4.0 software was used. The sensitivity of the analysis was validated by serial

dilution spiked-in samples of patients BM MNC. Our validation experiment revealed that for less than 5% of cells containing a mutation the Sequenom assay could not confidentially predict the presence or absence of a mutation (data not shown).

For the analysis of purified peripheral mature and xenotransplanted cells, we directly lysed the cells in 4µl of D2 lysis buffer from single cell REPLI-g kit (Qiagen) and the DNA was amplified according to manufacturer's instructions[17,18] prior to droplet digital PCR analysis. PCR reaction mixture preparation, droplet generation procedures, droplets analysis for emission in the HEX or FAM fluorescent signal channels using QX200 Droplet Digital PCR System (Bio-Rad, Berkeley, CA, USA) and QuantaSoft version 1.15 (Bio-Rad), and validation experiments are described in detail in supplementary methods.

Xenograft transplantation

NSG mice 8-10 weeks of age were given sublethal irradiation by exposure of two doses of 1.25 Gy (Cs source) four hours apart. Cells were injected intra-femorally within 24 hours of the last irradiation dose. 475-20,000 purified stem and progenitor cells were injected per mouse. Human engraftment and lineage distribution were analyzed by flow cytometry 20-22 weeks after injection. Reconstitution less than 0.1% was considered to be below the specificity of the method as previously described.[19,20] See supplementary methods for flow cytometry analysis from NSG BM. All mice were bred and maintained at the Oxford Biomedical Services and all the experiments were done with the approval of the UK Home Office.

CellProfiler image analysis software to measure ring sideroblasts

RS counting from engrafted paraffin-embedded (FFPE) NSG femur legs was performed using the automated open-source program CellProfiler (http:// www.cellprofiler.org).[21] The original color images were converted into grayscale images from scanned FFPE sections using the Panoramic MIDI II scanner and Panoramic Viewer software (3D Histech, Budapest, Hungary).

The images were taken using an AxioCam MRm (Carl Zeiss, Oberkochen, Germany) at 40x magnification. Segmentation was performed by the program's automatic thresholding algorithm to identify objects that were darker than the surrounding environment; these objects were potential RS. Filters were used to exclude objects that were either too big or too small, which usually represented various staining artifacts or debris. Accepted RS were highlighted by blue borders. These output images were manually inspected as a measure of quality assurance, and they also provided guidance for optimizing the program settings. For each erythrocyte with RS morphology, five basic parameters were measured: RS area, perimeter, major axis, minor axis, and form factor. Form factor was calculated by the formula ($4 \times \pi \times \text{area} / \text{perimeter}^2$) as a measurement of 'roundness.' It equals unity (1) for perfectly round objects, and decreases to 0 for more irregular or elongated objects. Image segmentation was done by manually picking a few representative RS, which served as color references and were processed by the program's proprietary algorithm.

Statistical analysis

Statistical analysis was performed using GraphPad Prism 7 software. For individual comparisons nonparametric Mann-Whitney test was used and p values less than 0.05 were considered significant.

Results

Patient characteristics

In total, we used BM samples from 40 patients with MDS-RS selected from the Karolinska Institutet MDS biobank for the various analyses. All had a normal karyotype; thirty-nine patients were *SF3B1* mutated and one *SF3B1* wild-type. Additional mutations found in these patients, as well as their clinical characteristics are shown in Table 1.

Functional characteristics of MDS-RS stem and progenitor cells

To gain information regarding the frequencies of the most primitive stem cells in MDS-RS patients we used flow cytometry based on previously described immunophenotypic marker protocols.[20,22-26] We isolated phenotypically defined HSCs ($7AAD^-Lin^-CD34^+CD38^-CD90^+CD45RA^-$), common myeloid progenitors (CMPs; $7AAD^-Lin^-CD34^+CD38^+CD90^-CD123^+CD45RA^-$), granulocyte-macrophage progenitors (GMPs; $7AAD^-Lin^-CD34^+CD38^+CD90^-CD123^+CD45RA^+$) and megakaryocyte-erythroid progenitors (MEPs; $7AAD^-Lin^-CD34^+CD38^+CD90^-CD123^-CD45RA^-$) from primary BM aspirates and compared stem/progenitor-cell immunophenotypes from 9 primary MNC MDS-RS samples with those from 4 healthy subjects. The immunophenotypic gating strategy, illustrated in Figure 1A, was validated by post FACS-sort purity analysis (Figure S1). The size of the $Lin^-CD34^+CD38^-CD90^+CD45RA^-$ HSC compartment in the MDS-RS patients, representing on average 0.13% of total BM cells (Figure 1B) was comparable to that in healthy NBM (0.08%, p=0.6). Neither were there any significant differences between the MDS-RS and healthy erythroid and myeloid progenitor compartments (Figure 1B).

The MDS-RS CMP, GMP and MEP subpopulations revealed normal capacity to generate colonies with mixed, myeloid- and erythroid-restricted lineage potentials respectively, but the efficacy of GMPs and MEPs to generate myeloid and erythroid colonies was significantly reduced as previously reported[22] (Figure 1C). MDS-RS erythroid BFU-E (burst forming unit-erythroid) colonies were characterized by poor hemoglobinization when compared to BFU-E colonies derived from normal healthy control individuals (Figure 1D). We then investigated the self-renewal potential *in vitro* of MDS-RS stem and progenitor cells using LTC-CFCs as an assay for stem cell activity,[20,27] and compared them with healthy NBM. LTC-CFCs activity in MDS-RS was significantly reduced but restricted to the MDS-RS HSC population, with no LTC-CFCs activity in any of the lineage restricted cell populations investigated (CMPs, GMPs and

MEPs; Figure 1E), thus suggesting that the self-renewal potential in MDS-RS is confined to the primitive stem cell compartment.

Initiating *SF3B1* spliceosome lesions originate from HSCs and are retained during differentiation

Computational prediction in the 39 cases studied of MDS-RS patients with one or more recurrent driver mutations based on targeted sequencing data (Figure 2A), demonstrated that the *SF3B1* mutation occurred alone in 14 cases, was predicted to be the first event in 10 cases, and to be secondary to other oncogenic mutations in only 3 cases. The remaining 12 cases were inconclusive as the computational analysis failed to reliably unravel the sequential acquisition pattern data (Figure S2). We also studied *in vitro* cultured individually picked LTC-CFC derived colonies from FACS purified stem cells and also colonies generated by purified progenitor cells. As expected, we were able to identify the *SF3B1* mutation at the HSC level from LTC-CFCs in all 7 *SF3B1* mutated patients (Figure 2B). These findings further support that recurrent *SF3B1* mutations typically target the rare self-renewing HSC compartment in MDS-RS. Next, we extended this analysis also to FACS purified stem and progenitor cells which were investigated for the presence of the *SF3B1* mutation using Sequenom analysis.[28] In agreement with the LTC-CFC results, in the 4 MDS-RS patients examined the *SF3B1* mutation could be backtracked to the HSC compartment, and was also found in downstream GMPs and MEPs but not in PB T-cells (Figure 2C). In order to further explore the potential multipotent (lymphomyeloid) HSC origin of *SF3B1* mutations in MDS-RS we next performed pyrosequencing of FACS-purified pro-B ($CD34^+CD19^+$) cells (Figure 3A, Figure S3A), which were found to be reduced in MDS-RS BM compared to healthy controls (3.8-fold reduction, $p<0.05$) (Figure 3B). In four of five MDS-RS patients analyzed, the *SF3B1* mutation was distinctly present in highly purified $CD34^+CD19^+$ BM progenitors (Figure 3C). In contrast, in the same patients, the involvement of mature B cells was at or below detection level (Figure 3C-D; Figure S3B), in agreement with previous studies.[12,13]

However, in one MDS-RS case (patient 4) harboring both *SF3B1* and *TET2* mutations, also mature B cells were highly clonally involved at diagnosis, and the allelic burden of both mutations increased with time in myeloid as well as B cells (Figure 3E, Figure S4, Table S1). The *SF3B1* mutation was not detected in T-cells, in any of the MDS-RS cases examined. Therefore, *SF3B1* mutations target lymphomyeloid HSCs in MDS-RS, and appear to negatively impact on lymphoid development.

In vivo ring sideroblasts formation from *SF3B1*-mutated MDS-RS HSCs

In order to assess the *in vivo* MDS-RS propagating ability of distinct MDS-RS stem and committed progenitor subsets, HSCs, CMPs, GMPs and MEPs were purified from 2 MDS-RS patients (Patients 4 and 5) and transplanted into NSG mice, and their ability to give sustained engraftment was analyzed after 20-22 weeks. In both cases, transplanted HSCs but not CMPs, GMPs or MEPs resulted in sustained myeloid and B cell engraftment (Figure 4A-B). Sensitive mutation detection analysis by droplet digital PCR established the *SF3B1* and *TET2* mutation clonal involvement of the myeloid cells reconstituted by the HSCs from patient 4 (Figure 4C, Table S2, Figure S5). In both of these cases as well as in two other cases (Patients 11 and 13), characteristic RS developed in the BM of NSG mice transplanted with *SF3B1*-mutated HSCs, while no RS were detected in mice transplanted with the progenitor cells from the same patients or in mice with engraftment following transplantation of healthy HSCs (Figure 4D-F). Importantly, since we in agreement with the known mutually exclusive expression of CD45 and GPA in normal erythroid development[29] found ring sideroblasts in *SF3B1*-mutated MDS-RS patients to be exclusively $CD45^{-}GPA^{+}$(Figures S6 and S7), we investigated the whole BM of transplanted NSG mice for the presence of RS.

The percentage of RS in total nucleated cells in the BM of the engrafted mice was calculated using CellProfiler image analysis software and ranged from 1.5-13.1% (Figure 4F) hence,

demonstrating robust *in vivo* generation of RS from transplanted MDS-RS *SF3B1* mutated HSCs in NSG mice.

Discussion

Herein, we provide phenotypic and functional evidence that the most primitive lymphomyeloid HSCs ($Lin^-CD34^+CD38^-CD90^+CD45RA^-$) represent the origin of the mutated *SF3B1* clone in MDS-RS, and also represent the rare MDS-RS propagating cells. In all the samples studied, we identified the *SF3B1* mutation in the majority of the *in vitro* generated colonies from LTC-CFCs, compatible with the driver mutation *SF3B1* providing HSCs in MDS-RS with a considerable clonal advantage at the HSC level. However, it is important to highlight the co-existence of wild-type LTC-CFCs, which could represent a potential therapeutic approach to change the balance of mutated versus wild-type HSCs. By contrast self-renewal potential *in vitro* and *in vivo* was not observed by any of the committed progenitor populations, suggesting that only the rare HSC compartment can propagate the *SF3B1*-mutated RS clone in the long-term.

Previous studies of MDS-RS found that the B cell lineage was not part of the *SF3B1* clone,[12,13] failing to support that *SF3B1* mutations in MDS-RS target lymphomyeloid HSCs. Also in our studies, in all cases but one did we find mature B cells to be minimally or not involved in the S*F3B1* mutated clone. In contrast, in the same patients we found definitive evidence for involvement at the early $CD34^+CD19^+$ Pro-B cell stage. Together with high clonal involvement at the $Lin^-CD34^+CD38^-CD90^+CD45RA^-$ HSC level, these findings provide evidence for S*F3B1* targeting lymphomyeloid HSCs in MDS-RS, and at the same time suggest that the S*F3B1* mutation and/or accompanying genomic lesions negatively impact on B-lymphoid development. This seems to contrast with the observation in Chronic Lymphocytic Leukemia (CLL), in which the same *SF3B1* mutations do not appear to negatively impact on the B cell lineage.[30] This might reflect that *SF3B1* mutations in CLL, unlike in MDS-RS, typically are subclonal, suggesting that they are secondary to other driver lesions in CLL.[31,32] Moreover, the impact of *SF3B1*

mutations on the B cell lineage might be affected by the context of co-occurring driver mutations, which are distinct in MDS-RS and CLL. Finally, *SF3B1* mutations might target an earlier and/or distinct progenitor in MDS-RS than in CLL.

Also our consistent finding of the T lymphoid lineage not being part of the S*F3B1* clone is in line with recurrent S*F3B1* mutations being incompatible with normal lymphoid development. However, similar findings have been made in del5q MDS,[33] and might also reflect that T cells are long lived and T-lymphopoiesis being inactive in the elderly.[34-36]

Our computational prediction analyses are most compatible with a model in which mutations in *SF3B1* in MDS-RS typically is the initiating recurrent driver mutation targeting HSCs in most MDS-RS cases, in accordance with previous studies.[5,20] Importantly, our finding that *SF3B1* recurrent mutations target the rare $Lin^-CD34^+CD38^-CD90^+CD45RA^-$ HSCs and provide these with a competitive advantage over healthy HSCs seems to be the rule rather than exception in low- to intermediate-risk MDS,[20] most likely reflecting that MDS-initiating lesions do not typically confer self-renewal properties to downstream progenitors. Also, most MDS-initiating mutations targeting $Lin^-CD34^+CD38^-CD90^+CD45RA^-$ HSCs seem to negatively affect lymphoid development, as our studies are among the few that have been able to demonstrate significant clonal involvement also of lymphoid lineages.[33]

Notably, analysis of bone biopsies of NSG mice established that transplanted *SF3B1* mutated MDS-RS HSCs had differentiated into the erythroid lineage and generated morphological distinct RS, the hallmark of MDS-RS. While RS engraftment was not reported in a previous study in which purified HSCs from a *SF3B1* mutated MDS-RS case gave myeloid engraftment, this would have been missed since apparently only engraftment of cells expressing the common leukocyte CD45 antigen was investigated,[12] whereas the mature erythroid lineage including RS do not express CD45. [29]

While initial studies suggested that *SF3B1* haploinsufficient mice have increased frequencies of RS in the BM,[37,38] subsequent studies of *SF3B1*^{K700E} knock-in mice as well as *SF3B1*$^{+/-}$ mice failed to confirm an increase in characteristic RS or circulating siderocytes despite of other signs of progressive macrocytic anemia and myelodysplasia.[39-42] This is consistent with no increases in RS also in mouse models of other mutations resulting in sideroblastic anemia in human.[43] The cellular and molecular basis for this possible species difference remains unclear. It cannot be excluded that this might be explained by the requirement for additional genetic or epigenetic mutations and dysregulation to develop the full phenotype and clinical picture of RS anemia. Regardless, the fact that we found characteristic RS to develop in NSG mice from transplanted *SF3B1*-mutated HSCs from MDS-RS patients, but not healthy human subjects, highlights the potential usefulness of exploring the cellular and molecular basis as well as therapeutic targeting of MDS-RS in this *in vivo* xenograft model. Moreover, it suggests that the difference observed in development of RS in *SF3B1*^{K700E} knock-in mice and *SF3B1* mutated MDS-RS patients, is likely to be explained by a hematopoietic intrinsic rather than extrinsic mechanism.

In conclusion, our findings provide evidence of a lymphomyeloid stem cell origin of the *SF3B1* mutation in MDS-RS patients and a novel *in vivo* platform for mechanistically and therapeutically exploring MDS-RS.

Acknowledgements

The authors thank the WIRM flow cytometry facility (supported by Knut and Alice Wallenberg Foundation) for technical assistance with the sorting experiments at Karolinska Institute (KI), Johanna Ungerstedt for BM sampling from healthy controls (KI), Asmaa Ben Azenkoud for processing the BM MNC and biobanking (KI), Gunilla Waldin for handling of clinical data for the patients (KI), Onima Chowdhury for technical support with the xenotransplantation experiments performed at the Weatherall Institute of Molecular Medicine, and Raoul Kuiper and Tarja Schröder from the core facility for morphological phenotype analysis (FENO) at the department

of Laboratory Medicine (KI) for help during mice histopathology. E.H.L. is funded through The Swedish Cancer Society (Cancerfonden) 150269, The Cancer Research Foundations of Radiumhemmets (Radiumhemmets Forskningsfonder) 151103, and the Swedish Research Council (Vetenskapsrådet) 521-2013-3577. S.E.W.J. is supported by an international recruitment grant from the Swedish Medical Research Council, a grant from the Tobias Foundation and a grant from the Center for Innovative Medicine (CIMED) at the Karolinska Institute.

Authorship

Contribution: T.M.B performed and analysed experiments and wrote the manuscript. E.H.L. and S.E.W.J. designed the study and wrote the manuscript. M.D. and P.S.W. performed experiments, analysed results, and contributed to writing of the manuscript. I.D. performed parts of the sorting experiments. M.D., M.K., M.M. and E.P. were involved in the generation, analysis or meta-analysis of sequencing data. E.E. and S.C. performed experiments. M.T. and M.J. co-ordinated the sampling of healthy donors and biobanking. L.S. performed the pathology analysis. All authors read and approved the final manuscript.

Conflict-of-interest disclosure

The authors declare no conflict of interest.

References

1. Hellström-Lindberg E. Significance of JAK2 and TET2 mutations in myelodysplastic syndromes. *Blood Reviews*. 2010;24(2):83-90.

2. Yoshida K, Sanada M, Shiraishi Y, et al. Frequent pathway mutations of splicing machinery in myelodysplasia. *Nature*. 2011;478(7367):64-69.

3. Papaemmanuil E, Cazzola M, Boultwood J, et al. Somatic SF3B1 mutation in myelodysplasia with ring sideroblasts. *The New England journal of medicine*. 2011;365(15):1384-1395.

4. Delhommeau F, Dupont S, Della Valle V, et al. Mutation in TET2 in myeloid cancers. *The New England journal of medicine*. 2009;360(22):2289-2301.

5. Papaemmanuil E, Gerstung M, Malcovati L, et al. Clinical and biological implications of driver mutations in myelodysplastic syndromes. *Blood*. 2013;122(22):3616-3627.

6. Haferlach T, Nagata Y, Grossmann V, et al. Landscape of genetic lesions in 944 patients with myelodysplastic syndromes. *Leukemia*. 2014;28(2):241-247.

7. Malcovati L, Papaemmanuil E, Bowen DT, et al. Clinical significance of SF3B1 mutations in myelodysplastic syndromes and myelodysplastic/myeloproliferative neoplasms. *Blood*. 2011;118(24):6239-6246.

8. Makishima H, Yoshizato T, Yoshida K, et al. Dynamics of clonal evolution in myelodysplastic syndromes. *Nat Genet*. 2017;49:204-212.

9. McKerrell T, Park N, Moreno T, et al. Leukemia-associated somatic mutations drive distinct patterns of age-related clonal hemopoiesis. *Cell Reports*. 2015;10(8):1239-1245.

10. Conte S, Katayama S, Vesterlund L, et al. Aberrant splicing of genes involved in haemoglobin synthesis and impaired terminal erythroid maturation in SF3B1 mutated refractory anaemia with ring sideroblasts. *British journal of haematology*. 2015;171(4):478-490.

11. Cazzola M, Invernizzi R, Bergamaschi G, et al. Mitochondrial ferritin expression in erythroid cells from patients with sideroblastic anemia. *Blood*. 2003;101(5):1996-2000.

12. Mian SA, Rouault-Pierre K, Smith AE, et al. SF3B1 mutant MDS-initiating cells may arise from the haematopoietic stem cell compartment. *Nat Commun*. 2015;6:10004.

13. Mian SA, Smith AE, Kulasekararaj AG, et al. Spliceosome mutations exhibit specific associations with epigenetic modifiers and proto-oncogenes mutated in myelodysplastic syndrome. *Haematologica*. 2013;98(7):1058-1066.

14. Vardiman J, Thiele J, Arber D, et al. The 2008 revision of the World Health Organization (WHO) classification of myeloid neoplasms and acute leukemia: rationale and important changes. *Blood*. 2009;114(5):937-951.

15. Malcovati L, Karimi M, Papaemmanuil E, et al. SF3B1 mutation identifies a distinct subset of myelodysplastic syndrome with ring sideroblasts. *Blood*. 2015;126(2):233-241.

16. Papaemmanuil E, Gerstung M, Bullinger L, et al. Genomic classification and prognosis in acute myeloid leukemia. *New England Journal of Medicine*. 2016;374(23):2209-2221.

17. Brambati C, Galbiati S, Xue E, et al. Droplet digital polymerase chain reaction for DNMT3A and IDH1/2 mutations to improve early detection of acute myeloid leukemia relapse after allogeneic hematopoietic stem cell transplantation. *Haematologica*. 2016;101(4):e157-e161.

18. Shlush LI, Zandi S, Mitchell A, et al. Identification of pre-leukaemic haematopoietic stem cells in acute leukaemia. *Nature*. 2014;506(7488):328-333.

19. Dimitriou M, Woll PS, Mortera-Blanco T, et al. Perturbed hematopoietic stem and progenitor cell hierarchy in myelodysplastic syndromes patients with monosomy 7 as the sole cytogenetic abnormality. *Oncotarget*. 2016;7(45).

20. Woll PS, Kjällquist U, Chowdhury O, et al. Myelodysplastic syndromes are propagated by rare and distinct human cancer stem cells in vivo. *Cancer Cell*. 2014;25(6):794-808.

21. Carpenter AE, Jones TR, Lamprecht MR, et al. CellProfiler: image analysis software for identifying and quantifying cell phenotypes. *Genome Biology*. 2006;7(10):1-11.

22. Nilsson L, Edén P, Olsson E, et al. The molecular signature of MDS stem cells supports a stem-cell origin of 5q− myelodysplastic syndromes. *Blood*. 2007;110(8):3005-3014.

23. Manz MG, Miyamoto T, Akashi K, Weissman IL. Prospective isolation of human clonogenic common myeloid progenitors. *Proc Natl Acad Sci U S A*. 2002;99(18):11872-11877.

24. Murray L, DiGiusto D, Chen B, et al. Analysis of human hematopoietic stem cell populations. *Blood*. 1994;20(2-3):364-369.

25. Majeti R, Park CY, Weissman IL. Identification of a hierarchy of multipotent hematopoietic progenitors in human cord blood. *Cell Stem Cell*. 2007;1(6):635-645.

26. Steidl U, Rosenbauer F, Verhaak R, et al. Essential role of Jun family transcription factors in PU.1 knockdown-induced leukemic stem cells. *Nat Genet*. 2006;38(11):1269-1277.

27. Sutherland H, Eaves C, Eaves A, Dragowska W, Lansdorp P. Characterization and partial purification of human marrow cells capable of initiating long-term hematopoiesis in vitro. *Blood*. 1989;74(5):1563-1570.

28. Karimi M, Nilsson C, Dimitriou M, et al. High-throughput mutational screening adds clinically important information in myelodysplastic syndromes and secondary or therapy-related acute myeloid leukemia. *Haematologica*. 2015;100(6):e223-e225.

29. Malcovati L, Della Porta MG, Lunghi M, et al. Flow cytometry evaluation of erythroid and myeloid dysplasia in patients with myelodysplastic syndrome. *Leukemia*. 2005;19(5):776-783.

30. Wang L, Lawrence MS, Wan Y, et al. SF3B1 and other novel cancer genes in chronic lymphocytic leukemia. *The New England journal of medicine*. 2011;365.

31. Landau DA, Tausch E, Taylor-Weiner AN, et al. Mutations driving CLL and their evolution in progression and relapse. *Nature*. 2015;526(7574):525-530.

32. Quesada V, Conde L, Villamor N, et al. Exome sequencing identifies recurrent mutations of the splicing factor SF3B1 gene in chronic lymphocytic leukemia. *Nat Genet*. 2012;44(1):47-52.

33. Nilsson L, Åstrand-Grundström I, Arvidsson I, et al. Isolation and characterization of hematopoietic progenitor/stem cells in 5q-deleted myelodysplastic syndromes: evidence for involvement at the hematopoietic stem cell level. *Blood*. 2000;96(6):2012-2021.

34. Buckton K, Brown W, Smith P. Lymphocyte survival in men treated with x-rays for ankylosing spondylitis. *Nature*. 1967;214:470-473.

35. Galy A, Travis M, Cen D, Chen B. Human T, B, natural killer, and dendritic cells arise from a common bone marrow progenitor cell subset. *Immunity*. 1995;3(4):459-473.

36. Kondo M, Weissman IL, Akashi K. Identification of Clonogenic Common Lymphoid Progenitors in Mouse Bone Marrow. *Cell*. 1997;91(5):661-672.

37. Visconte V, Rogers HJ, Singh J, et al. SF3B1 haploinsufficiency leads to formation of ring sideroblasts in myelodysplastic syndromes. *Blood*. 2012;120(16):3173-3186.

38. Visconte V, Tabarroki A, Zhang L, et al. Splicing factor 3b subunit 1 (SF3B1) haploinsufficient mice display features of low risk Myelodysplastic syndromes with ring sideroblasts. *Journal of Hematology & Oncology*. 2014;7(1):89.

39. Obeng Esther A, Chappell Ryan J, Seiler M, et al. Physiologic expression of SF3B1 K700E causes impaired erythropoiesis, aberrant splicing, and sensitivity to therapeutic spliceosome modulation. *Cancer Cell*. 2016;30(3):404-417.

40. Mupo A, Seiler M, Sathiaseelan V, et al. Hemopoietic-specific SF3B1-K700E knock-in mice display the splicing defect seen in human MDS but develop anemia without ring sideroblasts. *Leukemia*. 2017;31:720-727.

41. Matsunawa M, Yamamoto R, Sanada M, et al. Haploinsufficiency of SF3B1 leads to compromised stem cell function but not to myelodysplasia. *Leukemia*. 2014;28(9):1844-1850.

42. Wang C, Sashida G, Saraya A, et al. Depletion of SF3B1 impairs proliferative capacity of hematopoietic stem cells but is not sufficient to induce myelodysplasia. *Blood*. 2014;123(21):3336-3343.

43. Pondarré C, Antiochos BB, Campagna DR, et al. The mitochondrial ATP-binding cassette transporter ABCB7 is essential in mice and participates in cytosolic iron–sulfur cluster biogenesis. *Human Molecular Genetics*. 2006;15(6):953-964.

Table 1: Clinical, hematologic, and cytogenetic characteristics of MDS-RS patients

Patient n.	Sex	Age	Hb (g/L)	Transfusion	SF3B1 mutation	Other mutations (targeted seq)	BM cellularity %	% RS	% Blasts
1	F	72	102	No	p.K700E	STAG2 (340del)	70	29	1
2	F	69	89	No	p.K700E	TET2 (p.F125fs)	60	24	4.5
3	F	83	88	Yes	p.K700E	TET2 (Q916*)	90	30	4
4	M	78	97	No	p.K666R	c-KIT, TET2 (R1404*, 690*)	50	39	3
5	F	69	93	No	p.H662Q	TET2 (H1881Y)	80	33	5.5
6	M	76	97	No	p.H662D	DNMT3A (W305*)	60	23	4.5
7	F	78	103	No	p.E622D	B-COR (R63K)	60	21	2
8	M	87	80	Yes	p.R625L	IDH2 (R172K)	70	22	2
9	M	81	106	No	p.E622D	None	60	33	2.5
10	F	65	77	No	p.K700E	PRPF40B (669D)	90	39	2
11	F	81	107	No	p.K700E	EZH2 (T306fs), DNMT3A (E285*)	70	85	0.5
12	M	64	132	No	p.N626D	None	50	42	5.5
13	M	70	117	No	no mutation	SRSF2 (95_103del)	90	73	1.5
14	F	71	98	Yes	p.K700E	TET2 (Q746X)	80	55	2
15	F	77	97	Yes	p.E622D	JAK2 (V617F)	100	77	1
16	F	80	115	No	p.K700E	DNMT3A (V296M)	50	36	2.5
17	F	60	113	No	p.K700E	None	100	25	1.5
18	M	79	108	No	p.E622D	DNMT3A (I643M)	80	16	2
19	F	54	125	Yes	p.K700E	DNMT3A (F868S)	90	10	0
20	M	67	97	Yes	p.K700E	None	65	35	0
21	M	67	100	Yes	p.K700E	None	60	40	1
22	M	68	101	No	p.K700E	TET2 (E1555fs*22)	70	40	0
23	F	74	106	No	p.K666T	None	70	20	2.5
24	M	76	107	No	p.N626D	TET2 (R1452*)	-	16	2

25	F	82	99	No	p.E622D	None	50	24	1.5
26	M	77	115	Yes	p.E666R	None	60	45	3
27	F	84	93	Yes	p.K700E	EZH2 (K661E)	40	33	2
28	F	75	107	No	p.K700E	None	40	28	1.5
29	F	76	105	No	p.Y623C	None	40	49	1.5
30	F	80	97	No	p.K700E	None	60	16	3.5
31	F	73	102	No	p.E666R	None	50	53	1
32	F	79	135	No	p.K700E	TET2 (Q958fs*14)	-	35	0
33	M	77	87	Yes	p.R625L	None	-	26	0
34	M	73	87	Yes	p.R625L	TET2 (F1300I), SMC3 (L836X)	-	16	2
35	M	64	101	No	p.K666R	DNMT3A (Y735C)	-	23	2
36	F	79	101	No	p.H662Q	IDH2 (C402Y), TET2 (T1122fs*8)	-	30	1
37	F	46	109	No	p.K700E	None	50	44	1
38	M	68	101	Yes	p.K700E	IDH2 (R140Q), EZH2 (R732I), ZRSR2 (E120fs*24)	-	16	1
39	F	77	111	Yes	p.K700E	RUNX1 (R107S)	-	31	2
40	M	49	121	No	p.T663I	TET2 (P319fs*28)	90	70	3

F, female; M, male; Hb, hemoglobin; BM cellularity, bone marrow cellularity; %RS, % of ring sideroblasts

Figure legends

Figure 1: **Analysis of hematopoietic stem and progenitor cells in MDS-RS.** (A) Representative FACS analysis of *SF3B1*-mutated MDS-RS BM (patient 4). Shown are FACS analyses of viable, lineage negative CD34-enriched cells further gated as CMPs (common myeloid progenitors; $7AAD^-Lin^-CD34^+CD38^+CD90^-CD123^+CD45RA^-$), MEPs (megakaryocyte-erythroid progenitors; $7AAD^-Lin^-CD34^+CD38^+CD90^-CD123^-CD45RA^-$), GMPs (granulocyte-macrophage progenitors; $7AAD^-Lin^-CD34^+CD38^+CD90^-CD123^+CD45RA^+$); and HSCs (hematopoietic stem cells; $7AAD^-Lin^-CD34^+CD38^-CD90^+CD45RA^-$). (B) Mean (SEM) frequencies of HSCs and progenitors in *SF3B1*-mutated MDS-RS patients (n=9) and healthy normal bone marrow (NBM; n=4). (C) Mean (SEM) erythroid and myeloid colony formation from purified CMPs, GMPs and MEPs from 8 MDS-RS patients and 4 NBMs. (D) Representative images of erythroid colony (BFU-E) from an MDS-RS patient and a healthy NBM control. Original magnification for light microscopy x 10. (E) LTC-CFC activity from HSCs, CMPs, GMPs and MEPs from MDS-RS patients (n=8) and healthy NBM controls (n=5). Results are mean (SEM) values for all patients and healthy controls, in each case derived from the mean of 3 technical replicates for each cell population and patient. * $p < 0.05$, ** $p < 0.005$.

Figure 2: Evidence for *SF3B1* mutations being initiating mutations targeting rare HSCs in MDS-RS. (A) Computational prediction of fraction of cells with identified genomic lesions, within total BM mononuclear cells from *SF3B1*-mutated MDS-RS patients based on variant allele fraction (VAF). Error bars indicate 95% confidence interval (CI). Shown are cases where *SF3B1* is the only identified recurrent mutation, *SF3B1* is predicted to be the first of multiple recurrent mutations, or *SF3B1* is predicted to be secondary to other mutation(s). Inconclusive results (overlapping 95% confidence intervals) are included in Figure S2. (B) Tracking of *SF3B1* mutations in individually picked HSC-derived LTC-CFCs or MEP- and GMP-derived CFCs. 7 *SF3B1* mutated and 1 *SF3B1* wildtype (WT) patients were analysed using pyrosequencing to

screen for identified *SF3B1* mutations in each case, and scored as positive (grey), negative (white) or inconclusive (I) (see supplementary methods for definitions and cut-offs). (C) Sequenom analysis from 4 MDS-RS samples of FACS-purified stem and progenitor cell populations to assess *SF3B1* VAF.

Figure 3: *SF3B1* mutations in lymphoid as well as myeloid progenitors in MDS-RS. (A) Representative FACS-analysis of BM MNCs for healthy NBM and *SF3B1*-mutated MDS-RS (Patient 6), showing gating strategy for viable $Lin^-CD34^+CD19^+$ Pro-B cells. (B) Mean (SEM) frequencies of Pro-B cells in *SF3B1*-mutated MDS-RS patients (n=9) and healthy NBM (n=4). (C) VAF of *SF3B1* mutations in MDS-RS pro-B cells (MDS-RS PROB, n=5) and mature peripheral blood B cells from MDS-RS (MDS-RS B cells, n=3) compared to MDS-RS bulk BM MNCs (n=5). Healthy NBM Pro-B cells (NBM PROB, n=4) were included as a negative control for the pyrosequencing. (D) Representative gating strategy for FACS purification of peripheral blood $CD3^+CD8^+$ T-cells, $CD19^+$ B-cells and $CD33/66B/15^+$ myeloid cells from MDS-RS patient 4. (E) VAF of identified mutations in FACS-purified peripheral blood myeloid, B- and T- cells from MDS-RS patient 4 at diagnosis and 16 months later, using ddPCR. Healthy normal DNA was negative as indicated by dotted line (<0.1%).

Figure 4: *In vivo* reconstitution of Ring Sideroblasts from MDS-RS HSCs. (A) Representative FACS gating strategy used for analysis of human myeloid ($CD33/CD66b/CD15^+$) and lymphoid ($CD19^+$) engraftment in xenotransplanted NOD/LtSz-scid $IL2R\gamma c^{-/-}$ (NSG) mice transplanted with healthy or *SF3B1*-mutated MDS-RS human stem and progenitor cells. The number of purified HSCs, CMPs, GMPs and MEPs transplanted into NSG mice was according to their relative ratios in the patient BM. Patient 4: 1400, 5000, 21000 and 1400 cells, and patient 5: 25000, 55000, 49300 and 25200 cells, respectively. Top panels show gating in a non-transplanted NSG mice (negative control); and bottom panel analysis in NSG mouse transplanted with MDS-RS HSCs from patient 4. (B) *In vivo* human B-lymphoid and myeloid

engraftment in BM of NSG mice 20-22 weeks post-transplantation of FACS-purified HSCs or indicated progenitors (mean values from 2-3 mice/cell population per patient) from 2 *SF3B1*-mutated MDS-RS. (C) Mean VAF in myeloid cells derived from patient 4 HSCs transplanted in NSG mice. (D) Prussian blue stains from sections of paraffin-embedded (FFPE) BM tissue from NSG mice with human reconstitution from healthy (upper-left), or *SF3B1*-mutated MDS-RS HSCs (upper-right; patient 5). Lower-left panel shows positive control from BM of MDS-RS patient; scale bar 50 μm. Lower right, characteristic prussian blue positive cells in BM of NSG mice transplanted with MDS-RS HSCs from patient 5; scale bar 10 μm. (E) Cytospins of erythroid cells purified from BM of patient 5 (Figure S6), stained with prussian blue; scale bar 20 μm. (F) % RS of total nucleated BM cells in BM of NSG mice transplanted with purified HSCs.

Figure 1

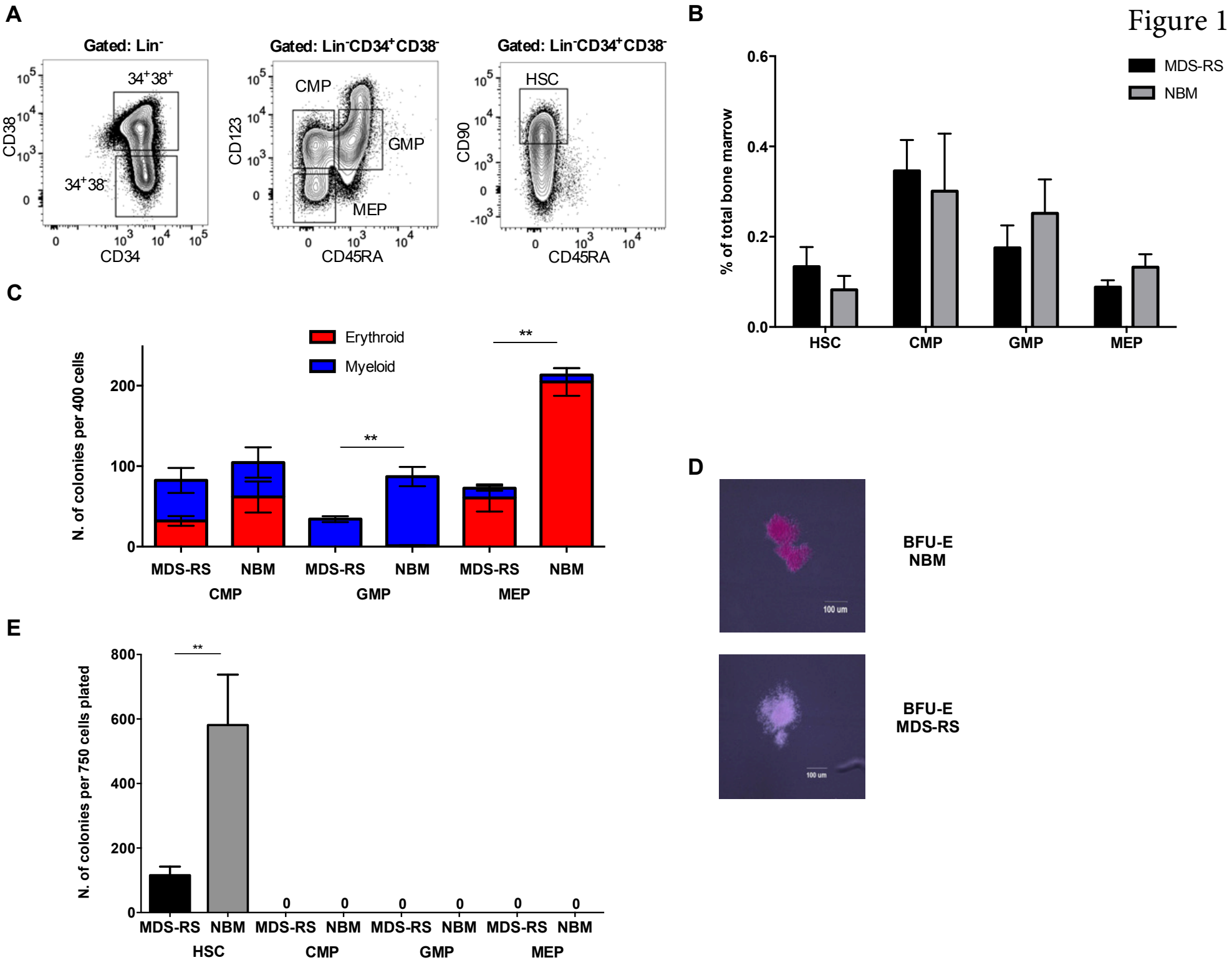
A
Gated: Lin-
34+38+
34+38-
CD38
CD34
Gated: Lin-CD34+CD38-
CMP
GMP
MEP
CD123
CD45RA
Gated: Lin-CD34+CD38-
HSC
CD90
CD45RA
B
MDS-RS
NBM
% of total bone marrow
HSC
CMP
GMP
MEP
C
Erythroid
Myeloid
N. of colonies per 400 cells
MDS-RS
NBM
CMP
GMP
MEP
D
BFU-E
NBM
BFU-E
MDS-RS
E
N. of colonies per 750 cells plated
HSC
CMP
GMP
MEP

Figure 2

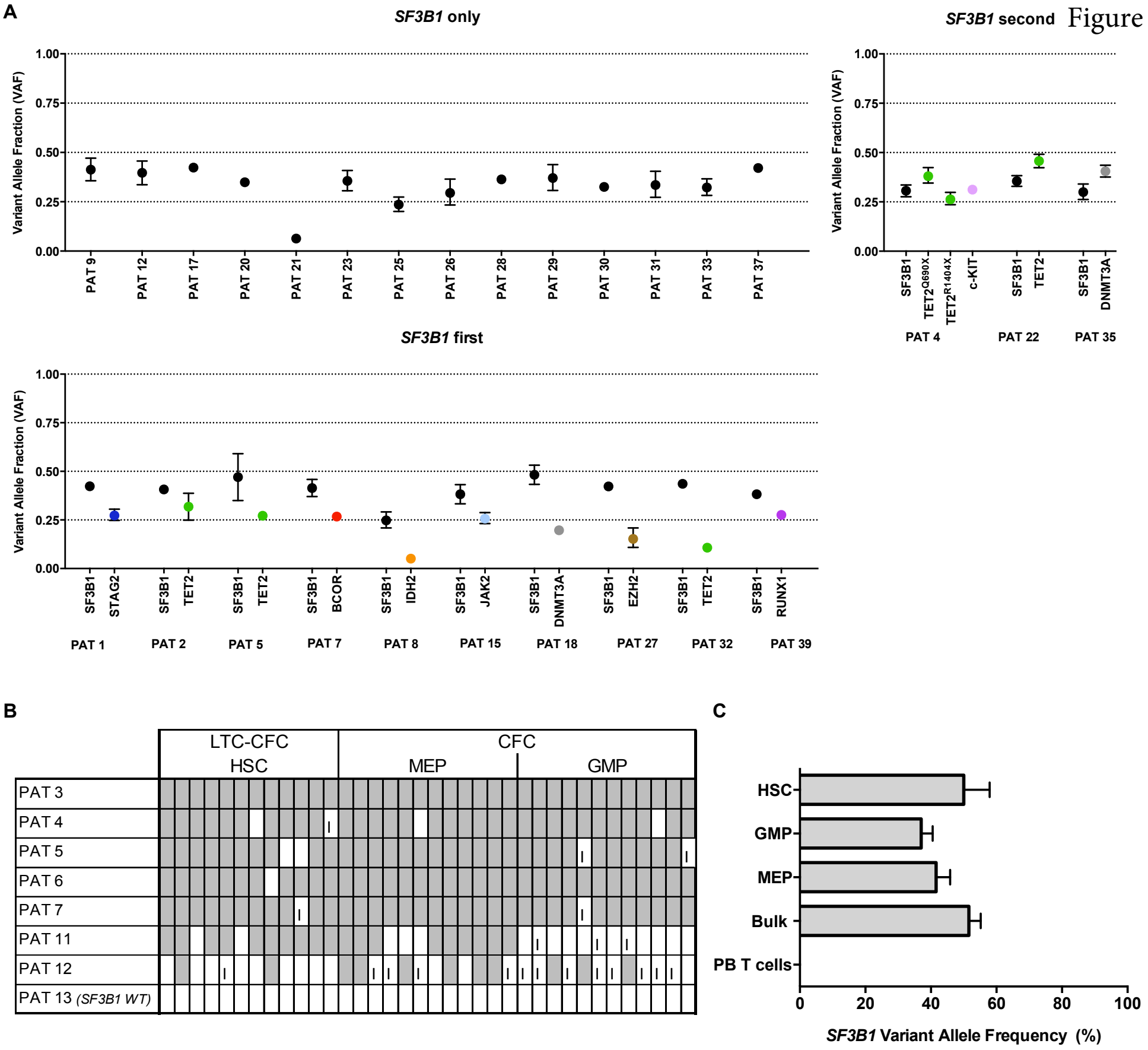
A
SF3B1 only
SF3B1 second
SF3B1 first
Variant Allele Fraction (VAF)
1.00
0.75
0.50
0.25
0.00
PAT 9
PAT 12
PAT 17
PAT 20
PAT 21
PAT 23
PAT 25
PAT 26
PAT 28
PAT 29
PAT 30
PAT 31
PAT 33
PAT 37
SF3B1
TET2Q690X
TET2R1404X
c-KIT
TET2
DNMT3A
PAT 4
PAT 22
PAT 35
SF3B1
STAG2
TET2
BCOR
IDH2
JAK2
DNMT3A
EZH2
RUNX1
PAT 1
PAT 2
PAT 5
PAT 7
PAT 8
PAT 15
PAT 18
PAT 27
PAT 32
PAT 39
B
LTC-CFC
HSC
CFC
MEP
GMP
PAT 3
PAT 4
PAT 5
PAT 6
PAT 7
PAT 11
PAT 12
PAT 13 (SF3B1 WT)
C
HSC
GMP
MEP
Bulk
PB T cells
0
20
40
60
80
100
SF3B1 Variant Allele Frequency (%)

Figure 3

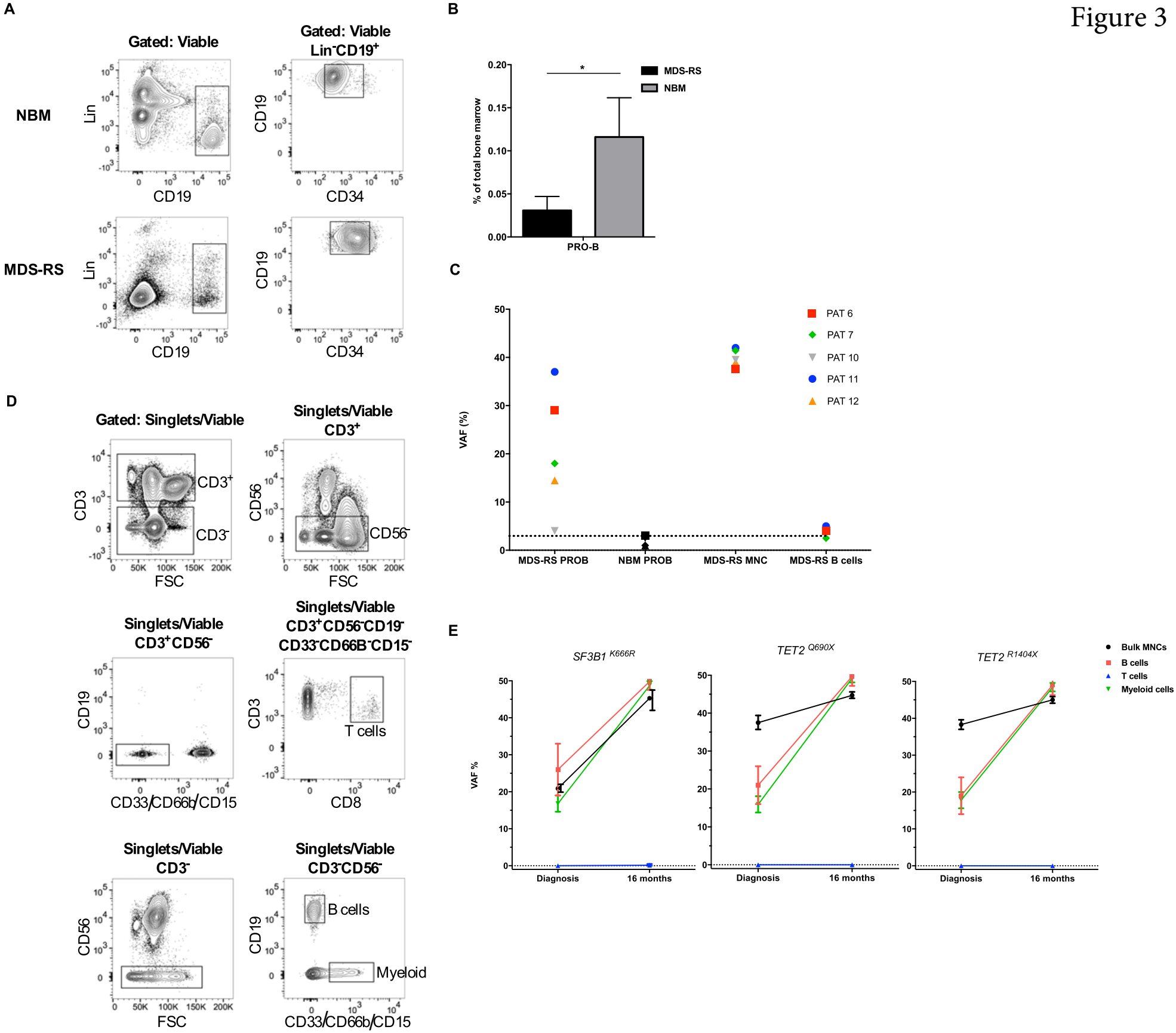
A
Gated: Viable
Gated: Viable Lin-CD19+
NBM
MDS-RS
Lin
CD19
CD34
B
MDS-RS
NBM
% of total bone marrow
PRO-B
C
PAT 6
PAT 7
PAT 10
PAT 11
PAT 12
VAF (%)
MDS-RS PROB
NBM PROB
MDS-RS MNC
MDS-RS B cells
D
Gated: Singlets/Viable
Singlets/Viable CD3+
Singlets/Viable CD3+CD56-
Singlets/Viable CD3+CD56-CD19- CD33-CD66B-CD15-
Singlets/Viable CD3-
Singlets/Viable CD3-CD56-
CD3+
CD3-
CD56-
T cells
B cells
Myeloid
FSC
CD33/CD66b/CD15
CD8
E
SF3B1 K666R
TET2 Q690X
TET2 R1404X
Bulk MNCs
B cells
T cells
Myeloid cells
VAF %
Diagnosis
16 months

Figure 4

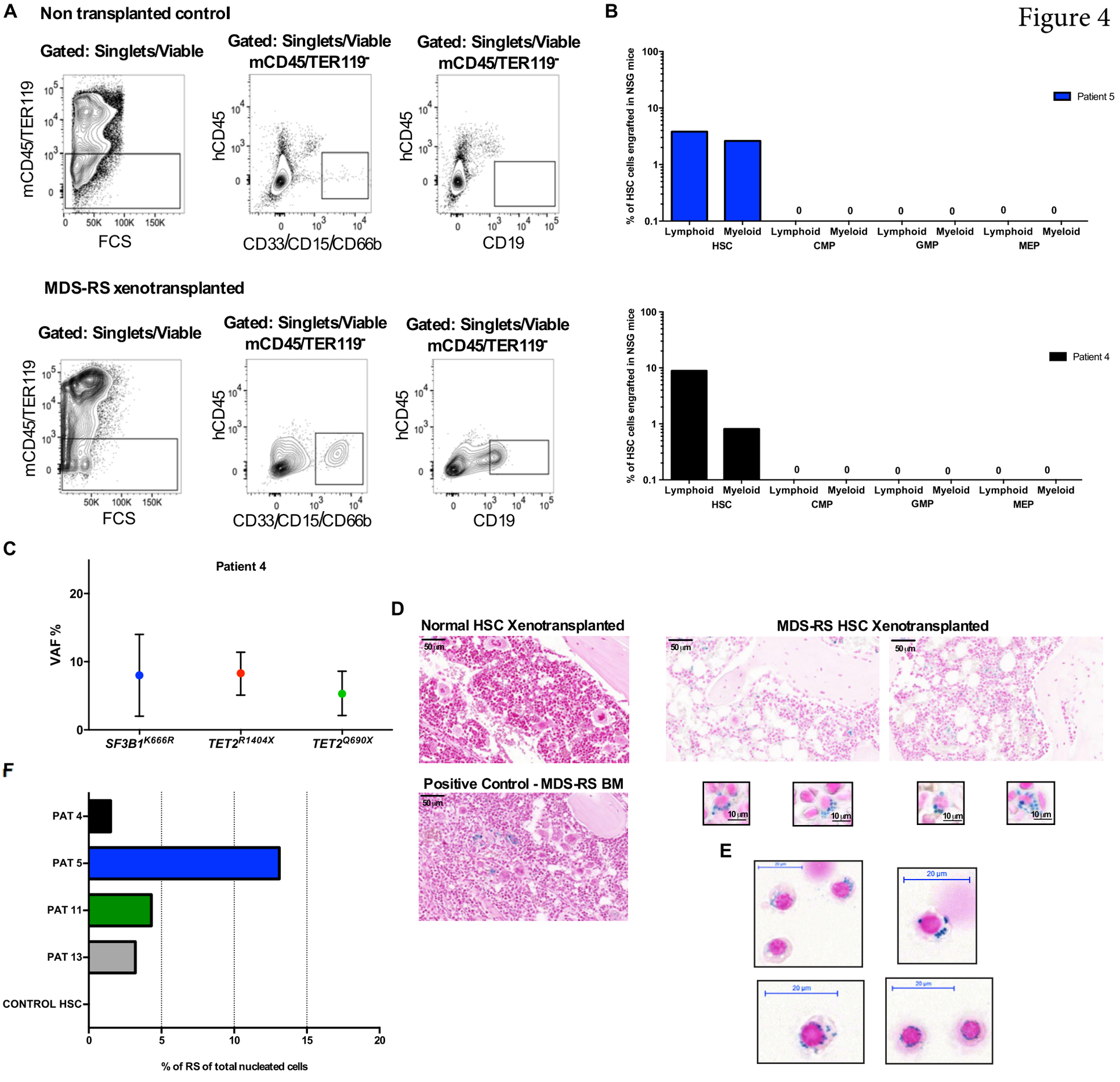
A
Non transplanted control
Gated: Singlets/Viable
mCD45/TER119
FCS
Gated: Singlets/Viable mCD45/TER119-
hCD45
CD33/CD15/CD66b
Gated: Singlets/Viable mCD45/TER119-
hCD45
CD19
MDS-RS xenotransplanted
Gated: Singlets/Viable
mCD45/TER119
FCS
Gated: Singlets/Viable mCD45/TER119-
hCD45
CD33/CD15/CD66b
Gated: Singlets/Viable mCD45/TER119-
hCD45
CD19
B
% of HSC cells engrafted in NSG mice
Patient 5
Lymphoid Myeloid Lymphoid Myeloid Lymphoid Myeloid Lymphoid Myeloid
HSC CMP GMP MEP
Patient 4
C
Patient 4
VAF %
SF3B1K666R
TET2R1404X
TET2Q690X
D
Normal HSC Xenotransplanted
MDS-RS HSC Xenotransplanted
Positive Control - MDS-RS BM
E
F
PAT 4
PAT 5
PAT 11
PAT 13
CONTROL HSC
% of RS of total nucleated cells

Prepublished online June 20, 2017;
doi:10.1182/blood-2017-03-776070

SF3B1-Initiating Mutations in MDS with Ring Sideroblasts Target Lymphomyeloid Hematopoietic Stem Cells

Teresa Mortera-Blanco, Marios Dimitriou, Petter S. Woll, Mohsen Karimi, Edda Elvarsdottir, Simona Conte, Magnus Tobiasson, Monika Jansson, Iyadh Douagi, Matahi Moarii, Leonie Saft, Elli Papaemmanuil, Sten Eirik W. Jacobsen and Eva Hellström-Lindberg

Blood (print ISSN 0006-4971, online ISSN 1528-0020), is published weekly by the American Society of Hematology, 2021 L St, NW, Suite 900, Washington DC 20036.